Original scientific paper

Application of biomimetic HPLC to estimate lipophilicity, protein and phospholipid binding of potential peptide therapeutics

Klara Valko*[1,2], Gabriela Ivanova-Berndt[3], Paul Beswick[3], Mark Kindey[4,5], Dorothy Ko[6]

[1]*Bio-Mimetic Chromatography Ltd, Business & Technology Centre, Stevenage, SG1 2DX United Kingdom*
[2]*Department of Biological and Pharmaceutical Chemistry, UCL School of Pharmacy London WC1N 1AX United Kingdom*
[3]*Bicycle Therapeutics Ltd, Cambridge, United Kingdom*
[4]*Department of Pharmaceutical Sciences, College of Pharmacy, University of South Florida, Tampa, FL, USA*
[5]*James A. Haley VAMC, Tampa, FL, USA*
[6]*Genervon Biopharmaceuticals LLC, Pasadena, CA, USA*

Corresponding Author: E-mail: klara_Valko@bio-mimetic-chromatography.com; Tel.: +447521 989558

Abstract

Peptide therapeutics are new modalities offering several challenges to drug discovery. They are generally less stable and permeable in vivo. The characterization of their lipophilicity cannot be carried out using the traditional in silico or wet octanol/water partition coefficients. The prediction of their in vivo distribution and permeability is also challenging. In this paper, it is demonstrated that the biomimetic properties such as lipophilicity, protein and phospholipid binding can be easily assessed by HPLC using chemically bonded protein and immobilized artificial membrane (IAM) stationary phases. The obtained properties for a set of potential therapeutic peptides with 3 to 33 amino acids have been analysed and it was found that similar characteristics of the properties could be observed as for small molecule drugs. The albumin binding showed correlation with their measured lipophilicity on the C-18 stationary phase with acidic peptides showing stronger than expected albumin binding. The (IAM) chromatography revealed peptide membrane affinity, which was stronger for positively charged peptides (containing arginine) and showed correlation to the alpha-1-acid glycoprotein (AGP) binding, which was also stronger for positively charged compounds. The in vivo volume of distribution and drug efficiency of the peptides have been estimated using the models developed for small molecules. One of the candidate linear peptides has been assessed in various cellular and in vivo assays and the results have confirmed the estimated cell partition and brain to plasma ratio. It can be demonstrated, that up to 21 amino acids, the peaks of the peptides obtained on the protein phase were symmetrical and narrow. The interaction of larger peptides with the protein stationary phases resulted in wide peaks showing multiple equilibrium processes with slow kinetics during chromatography. The larger peptides showed narrow and symmetrical peaks on the IAM column enabling the quantification of peptide - cell membrane interactions.

Keywords

Human Serum Albumin binding; Immobilized Artificial Membrane; chromatography, peptides, tissue binding, brain to plasma ratio

Introduction

Pharmaceutical and drug discovery companies are searching for new modalities outside the traditional small molecular drug space. Peptides, defined as having less than 50 amino acids, have been long recognized as potential therapeutics [1]. More than 140 peptides are now in clinical trials and more than 60 peptide drugs have been approved by FDA [2]. The therapeutic area ranges from antimicrobial to anticancer, but it is continuously expanding to new areas such as irritable bowel syndrome (linaclotide), Cushing's syndrome (pasireotide), myeloma (carfilzomib) and a few new peptides in Phase III clinical trials for osteoporosis and type II diabetes. It is worth mentioning that 6 peptides therapeutics out of 14 which are in Phase III clinical trials [1] are targeting central nervous system (CNS). Peptide therapeutics are able to inhibit protein-protein interactions (PPI) and are opening up numerous PPI targets for peptides and macrocyclic large molecules that are outside the traditional drug property space as defined by the Lipinski rule of five [3]. In general, peptides are selective and efficacious signalling molecules such as hormones, neurotransmitters, growth factors and ion channel ligands.

However, there are several issues with peptide therapeutics that have to be resolved. In spite of usually being water soluble, their oral absorption is compromised because of peptide hydrolysis occurring in the gastrointestinal tract. Proteolytic enzymes can decompose peptides quickly resulting in short plasma half-life even when the peptides are administered intravenously [4]. Approaches to extend the plasma half-life include substitution of cleavage sites by other amino acids, or to change the folding through enhancement of the secondary structure of the peptide. It is common to use lactam bridges, cyclisation and acylation. Another approach is to increase the serum albumin binding of peptide therapeutics to potentially increase the plasma half-life [4]. Therefore, measurements of albumin binding of potential peptide therapeutics are very important.

It is possible that pharmacologically active peptide therapeutics do not necessarily possess long plasma half-lives. For example, studies on SGX93 (Soligenix Inc) [5], a short peptide drug candidate that exhibited potential in oral mucositis in clinical trials showed a rapid degradation in plasma.

Due to their polar nature, peptides often have limited cell permeability. Cyclisation, reduction of the H-bond donor groups and other methods have been tried to identify cell-permeable peptides (CPP) [6-7]. There are three possible mechanisms by which peptides can enter into the cell: 1. the inverted micelle model; 2. direct penetration and 3. endocytic uptake [8]. When the target is intracellular it is important to design cell penetrating peptide therapeutics [9-10]. Various mechanisms on how peptides can enter into the cells have been reviewed by Madani *et al.* [11]. All of the aforementioned mechanisms require the peptide to have good affinity to the negatively charged membrane surface. Thus including arginine in the sequence could offer the potential to increases the cell permeability of the peptides [12]. Chromatography using immobilized artificial membrane (IAM) as a stationary phase [13-14] is a promising tool to measure the affinity of the peptide to the phospholipid membrane and relate it to cell permeability.

Another aspect of the rational design of peptide therapeutics is to improve their physicochemical properties, such as solubility and stability and to avoid aggregation. The stability of peptides can be improved by stabilizing α-helixes, salt bridges or lactam bridges. Therefore, several efforts have been published [6,15–19], for the synthesis of rigid or flexible cyclic peptides in relation to their cell permeability. Due to the low oral bioavailability of peptides, various formulation strategies have been developed such as liquid formulations. The search for a non-conventional administration route such as inhaled, topical or intravenous is a potential option to improve bioavailability.

Therefore, any predictive tool that can be used to estimate the *in vivo* distribution of potential peptide therapeutics would be very valuable.

Lipophilicity of molecules, expressed as an octanol/water partition coefficient (log *D*), has been used traditionally to model biological distribution processes [20]. It was found that the traditional octanol/water partition coefficient measurements were not suitable for the lipophilicity determination of peptides as peptides are charged and very polar and do not partition into octanol at all [21]. Moreover it is likely peptides could be concentrated on the interface between the octanol and the water. For instance, surface active peptides may help to form foams and emulsions that make the log *D* determination very difficult.

There is a study that describes a possible calculation method using 3D descriptors for the lipophilicity of the peptides in the octanol/water system [22]. *In silico* calculation software for log *D* provides very low calculated lipophilicities (below -5 and -10) in most cases. For example, in this study the calculated log *D* values using ACDLabs (Advanced Chemical Development Inc. Toronto, Canada) software for LP5 was -9.27 and for LP7 it was -9.84. On the other hand, these two compounds showed interactions with the IAM stationary phase and also had retention on the C-18 stationary phase.

Ermondi *et al*. [23] demonstrated that reversed phase chromatography could be used to assess and compare the lipophilicity of peptides. Others have also reported [24-25] that the lipophilicity of peptides is an important physicochemical property and that reversed phase chromatography can provide a tool to assess lipophilicity via retention time measurements. Biswas *et al*. [25] applied reversed-phase chromatography for lipophilicity assessment of amino acids and established an additivity rule of lipophilicity of peptides up to 15 amino acids. However, the additivity rule appeared to break down in larger peptides due to the secondary structure formation. *In silico* predictions of reversed phase retention may provide the possibility to assess the lipophilicity of peptides based on the retention coefficients for amino acids [26-28]. Gussakovsky *et al*. [29] analysed over 29 thousand tryptic peptides on the IAM.PC.DD2 stationary phase and compared the retention contribution of the amino acids with those from the C-18 columns. They found that amino acids containing positive charges such as arginine and lysine retain stronger on the IAM phase than on the C18 phase. They also determined that the amino acid contributions depended on the location of the amino acid in the sequence.

In this paper, we have investigated the retention behaviour of 20 potential peptide therapeutics, (one of them has been tested *in vivo*) including linear and bicyclic peptides on reversed-phase and biomimetic HPLC stationary phases such as human serum albumin (HSA), alpha-1-acid-glycoprotein (AGP) and IAM phases [14,30,32]. The measured properties have been analysed in comparison to marketed drugs' properties. The models developed for small molecules have been applied to the peptides to predict *in vivo* distribution and cell penetration.

Experimental

All chromatographic measurements were carried out on an Agilent 1100 series HPLC equipped with a UV-Diode Array Detector.

Lipophilicity measurements using C-18 stationary phase with acidic, neutral and basic pHs

The reversed phase fast gradient retention times have been measured using a Gemini NT C-18 column with the dimensions of 50 x 3 mm, particle size 5 μM with a 110 Å pore size (Phenomenex UK). The starting mobile phase was 0.01 M formic acid at pH 2.6 for low pH lipophilicity, 50 mM ammonium acetate buffers with pH adjusted to 7.4 and 10.5 by concentrated ammonia solution for neutral and basic pH lipophilicity

measurements, respectively. All reagents were HPLC grade obtained from Honeywell/Sigma-Aldrich, Germany. A 1.00 ml/min flow rate was applied. The acetonitrile gradient was from 0 to 100 % from 0 to 3.5 min then 100 % acetonitrile was kept until 4.5 min and then returned to 0 % at 4.7 min. The run time was 6 min. HPLC grade water and acetonitrile were obtained from Rathburn Chemicals Ltd, Walkerburn, UK. The gradient retention times were standardized using the Valko test mixture and the chromatographic hydrophobicity index (CHI) values as described previously [14,32]. The CHI values were converted to the octanol/water log D scale using Equation 1.

$$\text{CHI log } D = 0.0525 \text{ CHI} - 1.467 \tag{1}$$

In this way, the peptides lipophilicity can be compared to their octanol/water lipophilicity.

Measurements of membrane binding using immobilized artificial membrane (IAM) chromatography

For the measurements of the peptides interactions with phospholipids, the gradient retention times of the peptides have been measured using IAM.PC.DD2 100 x 4.6 mm column with 10 µM diameter and 300 Å pore size particles. The starting mobile phase was 50 mM ammonium acetate with the pH adjusted to 7.4. The acetonitrile gradient was applied from 0 to 90 % from 0 to 4.75 min and kept at 90 % until 5.25 min. From 5.25 to 5.5 min the acetonitrile concentration was dropped to 0. The mobile phase flow rate was 1.5 ml/min and the run time was 6 min. The retention times were standardized using the IAM calibration mixture as described previously [33]. The natural state of the phosphatidyl choline headgroup on the IAM stationary phase was tested using the six system suitability test compounds listed in Table 1. The CHI IAM values were converted to the octanol/water scale using Equation 2 [33].

$$\log K_{\text{IAM}} = 0.29*\exp(0.046 \text{ CHI IAM}+0.42) + 0.70 \tag{2}$$

The log K_{IAM} values express the membrane partition comparable to the octanol/water lipophilicity.

Table 1. The IAM system suitability test compounds and their expected CHI IAM values [14].

Compound	Acid/base	Typical retention time (min)	CHI IAM
Carbamazepine	Neutral	2.98	22.3
Colchicin	neutral	3.31	28.0
Warfarin	Acidic	2.62	16.4
Indomethacin	Acidic	3.15	25.3
Nicardipine	Basic	4.38	46.1
Propranolol	Basic	4.72	51.9

Protein binding measurements using biomimetic protein stationary phases

The peptides interactions with HSA and AGP have been measured using commercially available chemically bonded HSA (Chiralpak-HSA) and AGP (Chiralpak-AGP) HPLC columns with the dimensions of 50 x 3 mm with 5 µM particle size obtained from HiChrom Ltd, Reading, UK. The mobile phase was 50 mM ammonium acetate with the pH adjusted to 7.4. An iso-propanol gradient (HPLC grade, Rathburn Chemicals, Walkerburn, Uk) was used from 0 to 35 % from 0 to 3.5 min with a flow rate of 1.5 ml/min. The 35 % iso-propanol mobile phase was run till 4.5 min and then back to 0 % within 0.2 min. The run time was 6 min to allow re-equilibrate of the protein phase with the buffer. The retention times were standardized using the calibration set of compounds as described previously. Using the slope and intercept values from the calibration line the logarithmic retention times were converted to log k values that can be converted to % binding values (% HSA and % AGP) using Equation 3 [34].

$$\% \, \text{bound} = \frac{101 \cdot 10^{\log k}}{1 + 10^{\log k}}$$ (3)

Compounds studied

The linear peptides were obtained from GENERVON Biopharmaceuticals LLC (California, USA). These peptides were discovered as endogenous motor neuron trophic peptides that have a great potential to cure amyotrophic lateral sclerosis (ALS). The peptide with 6 amino acids (GM6) has already been tested in animal models of ALS and in Phase II human clinical trials. The analogues are marked as linear peptides (LP) with a serial number.

The bicyclic peptides were obtained from BiCycle TX, Cambridge, UK and are marked as BCP with a serial number. These are in the early stages of the drug discovery process.

Data analysis

The calculation of the biomimetic binding properties from the measured retention time values and estimating the *in vivo* distribution characteristics and cellular concentration [35] are based on the published models [36] and have been carried out using the Bio-Mimetic Chromatography Ltd propriety excel macros. The statistical analysis was carried out using JMP 13 (SAS Institute, USA) and the visualizations have been made by Stardrop software (Optibrium Ltd. Cambridge, UK).

Results and Discussion

The chromatographic peaks were symmetrical and narrow on the C18 and IAM stationary phases. A few examples are shown in Figure 1. However, larger peptides (containing more than 10 amino acids) showed wide peaks on the HSA column with a narrow peak at the dead time showing a size exclusion effect (Figure 2). Size exclusion occurs when large molecules cannot get into the pores of the stationary phases and elute with short retention times. It is worth mentioning that the Gemini NT C-18 column particle pore size is 110 Å and the IAM PC.DD2 column pore size is 300 Å and that would not produce a size exclusion effect for peptides below 3000 Da molecular weight. The good peak shape also suggests single interaction points between the peptide and the stationary phase on the C-18 and on the IAM stationary phases.

The broad peak observed for LP10 indicates multiple binding interactions with a slow kinetics between the peptide and the protein. The bicyclic peptides also showed broad peaks both for compounds with shorter and longer retention times. The peak shape of the linear peptides was narrow and symmetrical up to 21 amino acids.

Table 2 shows the measured data for 10 linear and 10 bicyclic peptides. The lipophilicity difference at acidic, neutral and basic pHs reveal the overall charges on the molecules at physiological pHs and whether the peptides are more positively or negatively charged.

It has been found that the pH dependence of the gradient retention times shows a similar profile to the pH dependence of the octanol/water distribution coefficients (log *D*) [37]. If the lipophilicity increased at a basic pH relative to the neutral pH lipophilicity, it would suggest that the peptide has more positive than negative charge. If the lipophilicity increases at an acidic pH, the peptide has more negative charge. It can be seen that the linear peptides are positively charged at physiological pH, while BCP1, BCP2 and BCP10 have more negative charge at physiological pHs. When plotting the CHI log *D* at pH 7.4 as a function of the molecular weight, we can see some trends for the linear peptides as shown in Figure 3.

Table 2. The measured protein binding (%HSA, log k HSA, %AGP, log k AGP), phospholipid binding (CHI IAM, log K IAM) and lipophilicity at three pHs (CHI log *D* 2.6, CHI log *D* 7.4, CHI log *D* 10.5) and phospholipid binding of the investigated linear (LP) and bicyclic peptides (BCP). The data of the known macrocyclic drug, cyclosporine is marked as CP.

Peptide	% bound HSA	log *k* HSA	% bound AGP	log *k* AGP	CHI IAM	log *K* IAM	CHI log *D* 2.6	CHI log *D* 7.4	CHI log *D* 10.5
LP1	7.85	-1.07	3.70	-1.42	5.47	1.27	-1.94	-0.54	-0.50
LP2	13.58	-0.81	6.85	-1.14	15.32	1.59	-0.75	-0.26	-0.23
LP3	13.15	-0.82	6.82	-1.14	17.46	1.69	-0.71	-0.14	-0.11
LP4	24.87	-0.49	61.24	0.19	43.04	3.90	-3.39	-0.14	0.22
LP5	20.73	-0.59	37.97	-0.22	42.25	3.78	-3.37	-0.17	0.19
LP6	77.54	0.52	49.58	-0.02	25.82	2.15	0.87	1.01	1.05
LP7	52.66	0.04	69.83	0.35	43.29	3.93	-0.15	0.77	1.07
LP8	95.75	1.26	74.92	0.46	37.47	3.17	0.18	0.83	0.82
LP9	98.97	1.69	89.84	0.91	43.80	4.01	1.18	1.59	0.61
LP10	99.07	1.71	87.83	0.82	37.66	3.20	1.17	1.60	0.61
BCP1	71.25	0.38	63.54	0.23	16.51	1.64	0.98	0.59	0.28
BCP2	88.58	0.85	1.31	-1.88	17.84	1.70	1.11	0.75	0.36
BCP3	19.03	-0.63	1.30	-1.89	16.10	1.63	0.24	0.54	0.25
BCP4	18.24	-0.66	35.68	-0.26	32.48	2.67	0.02	0.89	0.38
BCP5	92.92	1.06	73.34	0.42	39.98	3.48	0.89	1.79	1.54
BCP6	26.00	-0.46	2.69	-1.56	21.77	1.90	0.75	0.84	0.56
BCP7	9.24	-1.00	1.58	-1.80	18.08	1.71	0.57	0.65	0.36
BCP8	94.41	1.16	83.76	0.69	44.90	4.18	1.02	1.79	1.70
BCP9	82.29	0.64	32.81	-0.32	25.91	2.15	1.00	1.20	0.93
BCP10	96.28	1.31	49.46	-0.02	21.50	1.89	2.27	1.23	0.92
CP	91.00	0.97	60.9	0.18	51.33	5.38		5.31	
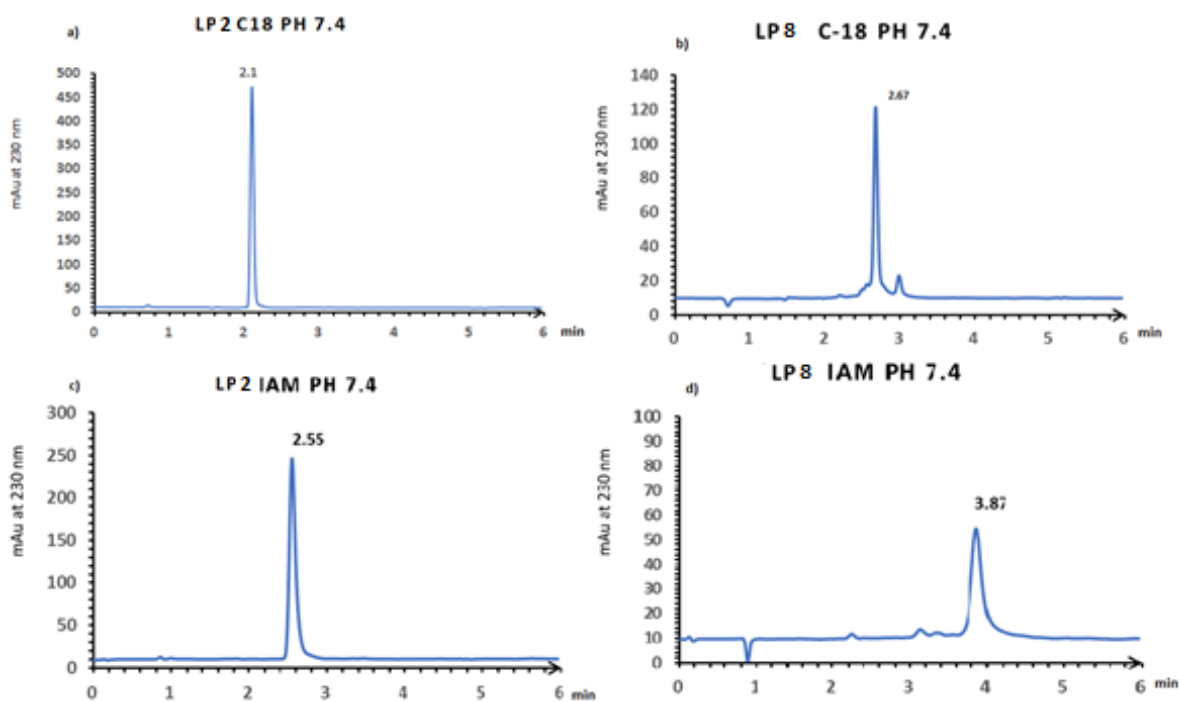
Figure 1. Chromatograms of LP2 and LP8 obtained on Gemini NX C-18 and IAM.PC.DD2 columns at pH 7.4. a) LP2 C-18 column, b) LP8 on C-18 column, c) LP2 on IAM.PC.DD2 column, d) LP8 on IAM.PC.DD2 column
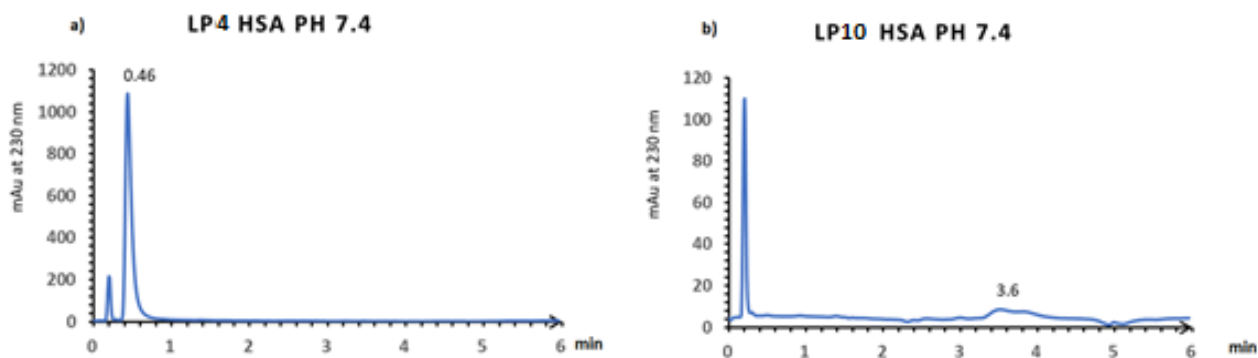
Figure 2. The chromatogram obtained on CHIRALPAK-HSA column for LP4 (a) and LP10 (b). Chromatographic conditions as described in the experimental section.
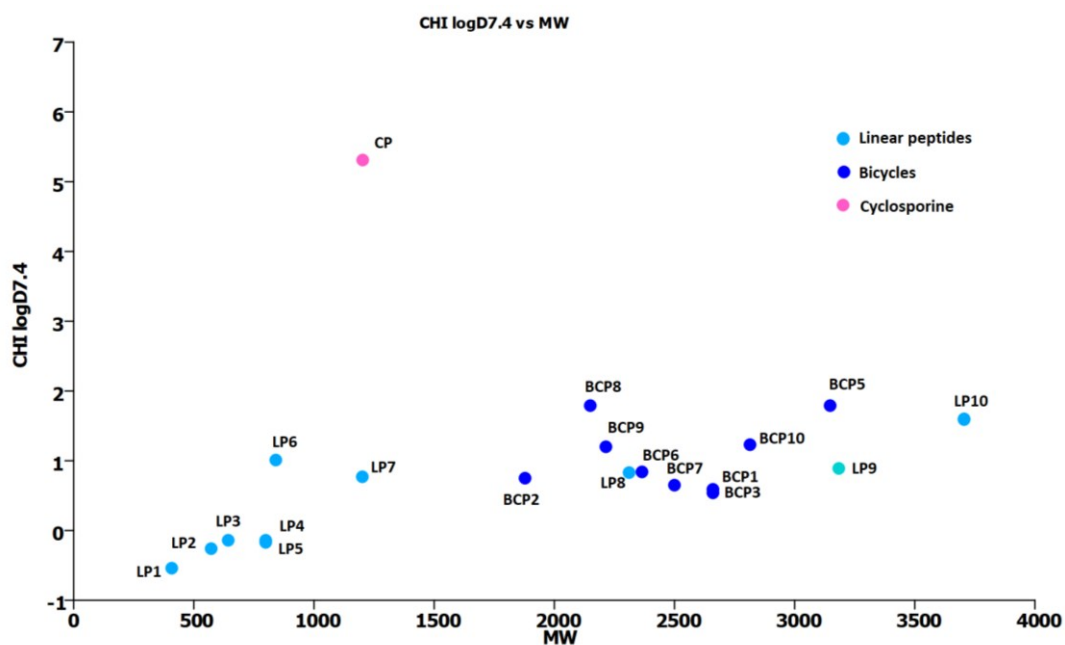

Figure 3. The CHI log $D_{7.4}$ values of the investigated peptides as a function of their molecular weight.
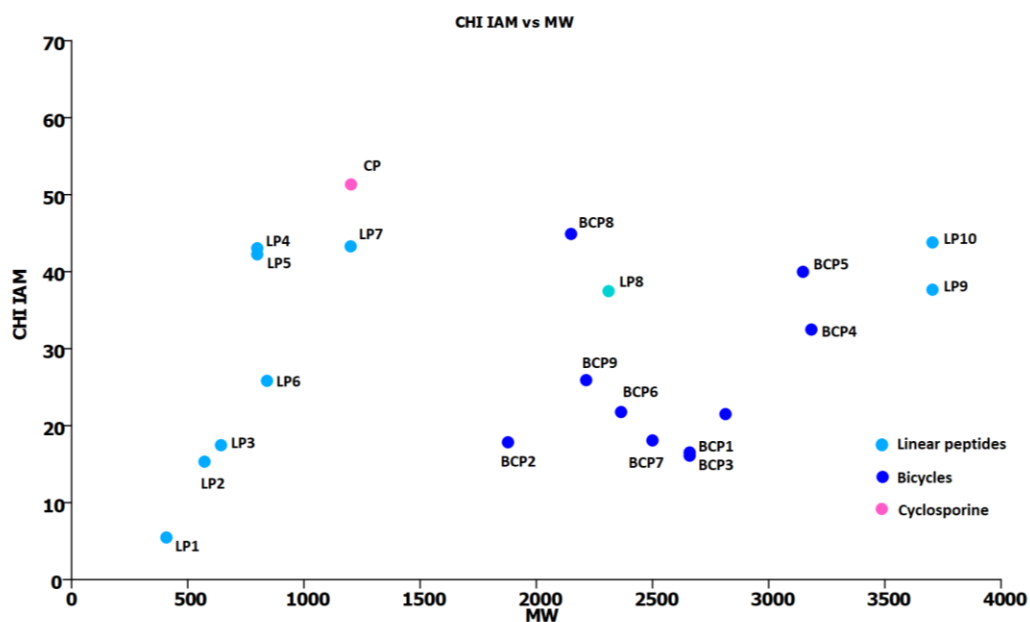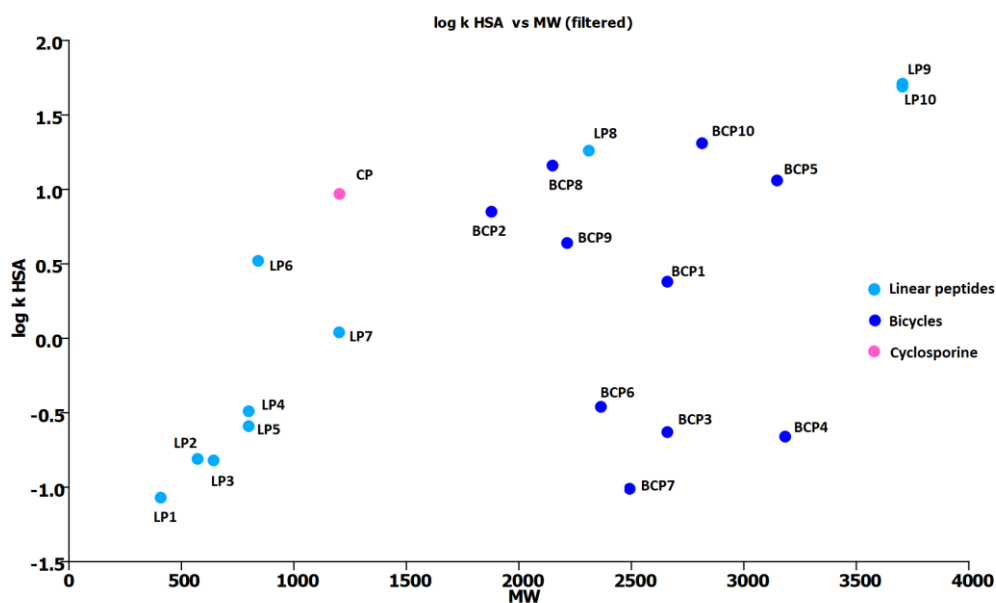

Figure 4. The CHI IAM values of the investigated peptides as a function of molecular weight.

Figure 5. The human serum albumin binding (log k_{HSA}) of the investigated peptides as a function of molecular weight.

From LP1 to LP10 the lipophilicity increases with size, while LP6 is slightly more lipophilic. With the linear peptides (LP8 and LP10) the lipophilicity increased but not proportionally with their larger molecular weight. This is in agreement with the finding that peptides with more than 16 amino acids start to fold and have secondary structure that may hinder the effect of certain amino acids on their lipophilicity [25].

Similar trends have been observed on the IAM.PC.DD2 stationary phase. The interactions with the phospholipid increased with the increasing number of amino acids as shown in Figure 4. The trend breaks for larger amino acids. Interestingly, the candidate peptide drug LP4 has stronger interactions with the phospholipids than the trend would show with the molecular weight due to its positive charge having two arginine in its sequence.

Figure 5 shows a similar plot for the human serum albumin binding in the function of molecular weight. For the linear peptides, as the amino acid number increase, the albumin binding increases up to LP8. Although the albumin binding is stronger for LP8 and LP10, it does not increase proportionally with the molecular weight. Some of the bicyclic peptides showed much weaker albumin binding, probably because the cyclization hindered several amino acids' interactions with the protein. Almost all of the bicyclic peptides showed wide peaks on the protein phases indicating multiple equilibria and sluggish kinetics.

Based on the measured biomimetic properties we have estimated the *in vivo* distribution behaviour of the investigated compounds. The model equations with the source references are listed in Table 3.

Table 4 contains the calculated total plasma protein binding (log k PPB), brain to plasma total concentration ratio (log k BB, Brain to plasma ratio), volume of distribution (log Vdss and Vdss L/kg), unbound volume of distribution (log Vdu, Vdu), drug efficiency (DEmax%) and estimated cell partition (Kpcell) data. The brain to plasma total concentration ratio has been calculated using the plasma protein binding (%PPB) and brain tissue binding (%BTB) models shown in Table 3 and described in [35]. From the %PPB and %BTB we can calculate the unbound fraction of the peptides (fu) in plasma and brain tissue using the equations listed in Table 3. According to the free drug hypothesis, the unbound concentration in plasma ($c_{u,plasma}$) and brain ($c_{u, brain}$) should be equal. The unbound concentrations can be expressed as fu

times c_{total} which leads to equation 4.

Table 3. The model equations used to derive estimated in vivo distribution (log V_{dss}, log V_{du}), drug efficiency (DE_{max}), brain tissue binding (log k_{BTB}), fraction unbound in brain and plasma (fu BTB and fu PPB), brain to plasma ratio (k_{bb}) and cell partition log K_{pcell}).

log K_{IAM} [33]	$= 0.29*e^{(0.026CHI(IAM)+0.42)} + 0.7$
Log k_{IAM} [33]	$=0.046*CHI(IAM) + 0.42$
log K_{HSA} [33]	$= e^{\log k(HSA)}$
log k_{HSA} [34]	$= \log(\%HSAbound/(101-\%HSA\ bound))$
Estimated log V_{dss} [33]	$= 0.44*\log K_{IAM} -0.22*\log K_{HSA} - 0.62$
Estimated log V_{du} [38]	$= 0.23*\log K_{HSA} +0.43*\log K_{IAM} - 0.72$
DE_{max} [39]	$= 100/V_{du}$
log k_{BTB} [36]	$=1.29*\log k_{IAM}+1.03*\log k_{HSA} - 2.37$
log k_{PPB} [36]	$=0.98*\log k_{HSA}+0.19*\log k_{AGP}+0.031*CHI\ \log D_{7.4}-0.20$
%BTB [36]	$=100*10^{\log k_{BTB}}/(1+10^{\log k_{BTB}})$
%PPB [36]	$=100*10^{\log k_{PPB}}/(1+10^{\log k_{PPB}})$
fu BTB and PPB [36]	$=(100-\%BTB)/100$ and $(100-\%PPB)/100$
K_{bb} [36]	$= fu_{PPB}/fu_{BTB}$
log K_{pcell} [35]	$=1.1*\log k_{IAM} - 1.9$

$$f_{u,\ plasma} \times c_{T,\ plasma} = f_{u,\ brain} \times c_{T,\ brain} \qquad (4)$$

Expressing the ratio of the total concentrations from equation 4, the equation for k_{bb} can be obtained and is listed in Table 3. Drugs that are able to go to the central nervous system (CNS) have significantly higher k_{bb} values than drugs that do not partition into the CNS. When k_{bb} is larger than 1 it means that the total concentration of the compound in the brain is higher than in the plasma. Therefore it is very likely that the compounds partition into the brain tissue (unless active transporters efflux the compound back to the plasma).

As the peptides easily decompose in plasma or blood under *in vitro* experimental conditions, it is very useful to estimate the peptides *in vivo* distribution behaviour considering them as intact molecules. The data in Table 4 reveals that there is a wide range of estimated total plasma protein binding in spite of the polar character of the peptides. The brain to plasma distribution ratio is generally low but some of the derivatives especially those that have positively charged amino acids, particularly with an arginine in the sequence, bind more strongly to phospholipids than to albumins thus increasing the expected brain to plasma total concentration ratio. The linear peptides are designed as candidate therapeutics for amyotrophic lateral sclerosis (ALS). Therefore brain penetration and cellular penetration are desired for these peptides. We can see from the measured data that LP4 (GM6 patented by Genervon) is predicted to have a good brain to plasma ratio. The volume of distribution is also quite large which means that it partitions into tissues extensively. Peptides that are more lipophilic at high pH (CHI log *D* at pH 10.5 is greater than CHI log *D* at pH 7.4) are predicted to have good cell penetration and the brain to plasma ratio is predicted to be greater than 1. This is because the phospholipid binding of positively charged peptides is stronger than that of the neutral molecules.

Table 4. Estimated *in vivo* distribution and tissue binding properties of the investigated peptides.

Peptide	% bound PPB	log k PPB	log k BB	Brain to plasma	log V_d	V_d L/kg	log V_{du}	V_{du}	% DE_{max}	K_{pcell}
LP1	6.85	-1.14	-0.03	0.93	-0.18	0.66	-0.10	0.80	124.83	0.07
LP2	13.36	-0.82	-0.05	0.88	-0.06	0.88	0.07	1.17	85.62	0.22
LP3	13.03	-0.83	-0.05	0.89	-0.01	0.97	0.11	1.27	78.44	0.28
LP4	36.55	-0.25	0.23	1.70	0.92	8.29	1.10	12.49	8.00	5.49
LP5	27.63	-0.42	0.20	1.58	0.88	7.62	1.03	10.82	9.25	5.01
LP6	85.20	0.73	-0.39	0.40	-0.08	0.82	0.59	3.89	25.70	0.74
LP7	68.47	0.32	0.34	2.21	0.84	6.96	1.21	16.23	6.16	5.66
LP8	98.17	1.54	-0.04	0.92	-0.04	0.91	1.46	28.62	3.49	2.87
LP9	99.99	2.00	-1.49	0.03	-0.08	0.82	2.25	176.76	0.57	6.00
LP10	99.99	2.00	-1.83	0.01	-0.47	0.34	1.92	84.13	1.19	2.93
BCP1	81.77	0.63	-0.25	0.25	-0.26	0.55	0.32	2.10	47.56	0.25
BCP2	84.04	0.70	0.19	0.36	-0.43	0.37	0.55	3.56	28.06	0.29
BCP3	14.84	-0.76	-0.01	0.88	-0.06	0.87	0.10	1.26	79.24	0.24
BCP4	25.70	-0.47	-0.03	0.94	0.40	2.51	0.55	3.51	28.47	1.60
BCP5	96.85	1.37	0.52	1.40	0.23	1.72	1.44	27.51	3.64	3.85
BCP6	23.29	-0.52	0.00	0.84	0.04	1.09	0.24	1.75	57.17	0.46
BCP7	7.46	-1.10	-0.02	0.94	0.01	1.03	0.10	1.26	79.11	0.30
BCP8	97.98	1.51	0.63	2.17	0.48	3.03	1.81	64.42	1.55	6.82
BCP9	87.21	0.80	0.11	0.43	-0.13	0.74	0.64	4.40	22.72	0.75
BCP10	97.97	1.51	-0.38	0.15	-0.64	0.23	0.94	8.77	11.40	0.45
CP	100	2.00	0.78	5.63	1.13	13.39	2.20	158	0.68	14.43

It is well known that cell penetration of peptides is usually impaired, as they are very hydrophilic and cannot go through the cell membrane with the same mechanism as small molecules [8].

However, endocytosis or micelle formation with phospholipids are possible cell penetration mechanisms which require strong interactions between the peptides and the phospholipid membrane.

The model for cell partition has been investigated using small molecule partition into HELA cells [35] and it was found that the IAM partition correlated better with intracellular concentration than other lipophilicity values. Therefore, the cell partition (Kp cell) has been estimated using the correlation with the IAM retention. Although the distribution models have been developed using the properties of small molecule marketed drugs based on their clinical data, it was supposed that the same models could be applied to peptides. Diaz-Eufracio et al [40] have compared the physicochemical property space of marketed peptide therapeutics with other marketed drugs and they found that they occupy similar property space. This study suggests that physicochemical properties of the peptides are not significantly different from small molecule marketed drugs and the drug-like properties can be described by the same physicochemical properties. They used calculated physicochemical properties. In this study, the measured physicochemical and biomimetic properties are compared with marketed drugs [36] and macrolides [41]. The marketed drugs were divided into inhaled and CNS group. A cyclic peptide natural product drug Cyclosporine (marked as CP) was also included in the analysis. Figure 6a shows the lipophilicity distribution and Figure 6b shows the IAM binding distribution of the peptides and the marketed drugs. It can be seen that the peptides are less lipophilic but their membrane partition (IAM binding) is within the range of other drug molecules.

a)

b)
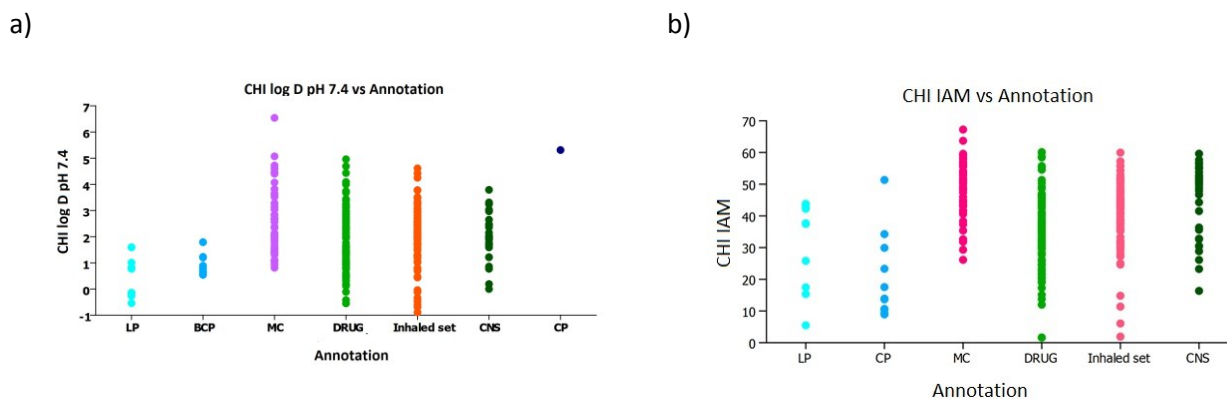
Figure 6. The lipophilicity (CHI log $D_{7.4}$) **(a)** and membrane partition (CHI IAM) **(b)**, of the peptides in comparison to macrocycle (MC), small molecule drugs (DRUG), inhaled drugs and drugs that can go to the central nervous system (CNS). CP stands for the natural cyclic peptide drug Cyclosporin.

The estimated brain to blood ratio (log k BB) and cell partition (log Kpcell) have been also compared based on the measured HPLC based biomimetic properties for the peptides, for the known drugs and for the macrolides as shown in Figure 7.

a)

b)
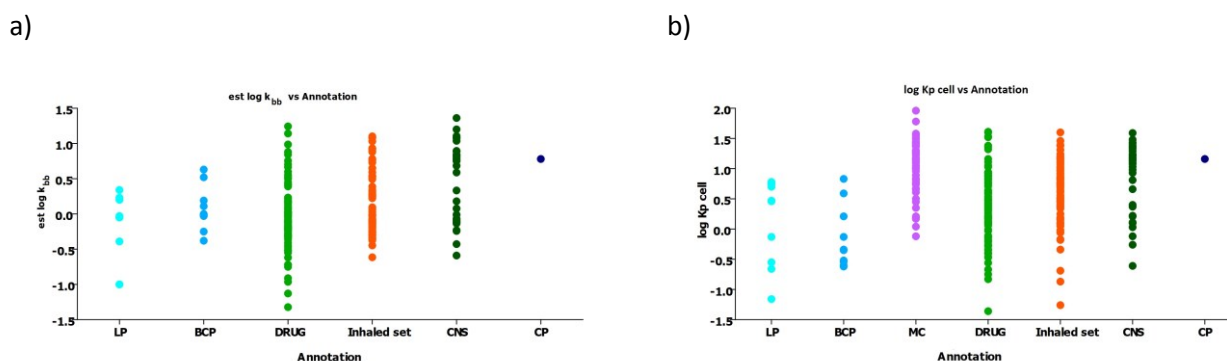
Figure 7. Distribution of the estimated brain to blood ratio (log k BB) **(a)** and cell partition (Kpcell) **(b)**, for the peptides in comparison to macrocycle (MC), small molecule drugs (DRUG), inhaled drugs and drugs that can go to the central nervous system (CNS). CP stands for the natural cyclic peptide drug Cyclosporin. (The macrocycles (MC) did not have all the data for estimating the log k BB therefore they are not shown in (a)

The interrelationship between the measured lipophilicity and biomimetic properties of the peptides have been investigated and a comparison made to the marketed drugs. In every respect, very similar relationships were observed. Figure 8 shows a good trend between the AGP and IAM binding of the compounds, as both bindings are influenced by the presence of the positive charge and general lipophilicity of the compounds. Both the linear and the cyclic peptides follow the same trend as the marketed drugs and macrolides.

One of the investigated compounds, Genervon's GM6 has been evaluated *in vivo* in a mouse model and also in humans. It has shown an effect in the SOD1 mouse model for ALS and in ALS patients [42] . As predicted, the peptide has been detected in the cells, especially in the motoneuron cells and was strongly associated with the cell membrane as confirmed using immune imaging technology. GM6 (LP4) has also been detected in the cerebrospinal fluid in mice after 4 hours.

These preliminary results encourage further studies of new modalities, such as peptides, cyclic peptides and macrocycles using biomimetic chromatographic methods and models.
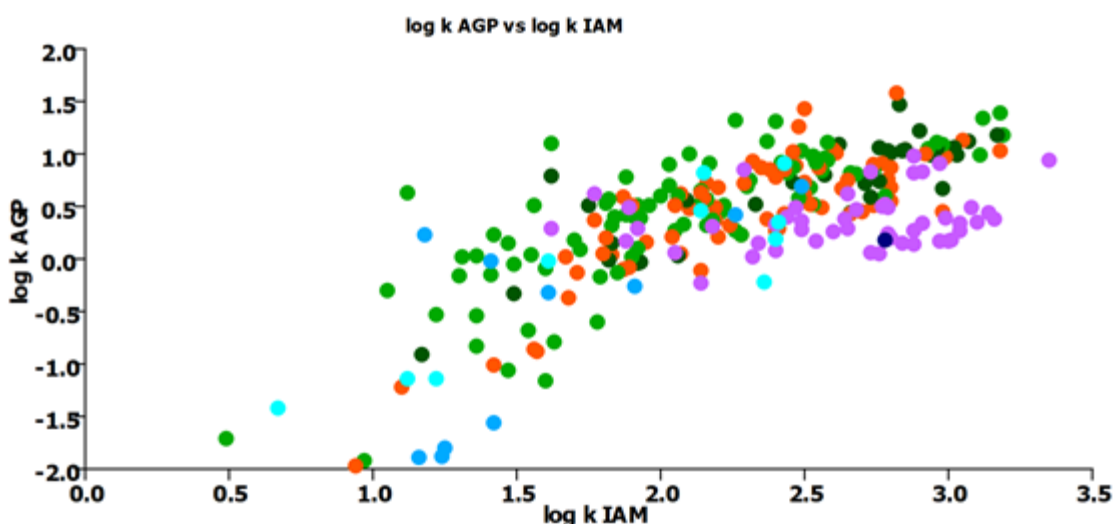
Figure 8. The trend between the alpha-1-acid glycoprotein binding (log k AGP) and phospholipid binding (log k IAM) for peptides, marketed drugs and macrolides. (Colour code is the same as in Figure 6 and 7.

Conclusions

The HPLC based physicochemical and biomimetic property measurements have been carried out on linear and bicyclic peptides. The measured properties, such as lipophilicity expressed as CHI log *D*, phospholipid binding expressed as CHI IAM (log k IAM) and protein binding (%HSA and %AGP) of selected linear and bicyclic peptides have been compared to the similar measured properties of marketed drugs. The lipophilicity, phospholipid binding and protein binding have been compared to the molecular weight of the peptides. It was found that larger molecular weight peptides had greater lipophilicity, phospholipid and protein binding; however, the trend was broken for bicyclic peptides and linear peptides above 16 amino acids. It suggests that the effect of the amino acids on the interactions with lipids and proteins are shielded for larger or cyclic peptides. The *in vivo* distribution models developed for small molecules have been applied for the first time to peptides. The estimation of good cell and brain penetration for LP4 (GM6), a linear peptide with 6 amino acids, has been validated in *in vitro* assays. Biomimetic HPLC measurements can, therefore, contribute to the design of peptide therapeutics with good drug-like properties.

References

[1] A.A. Kaspar, J.M. Reichert. Future directions for peptide therapeutics development. *Drug Discov. Today* **18** (2013) 807–817.

[2] K. Fosgerau, T. Hoffmann. Peptide therapeutics: Current status and future directions. *Drug Discov. Today* **20** (2015) 122–128.

[3] C.A. Lipinski, F. Lombardo, B.W. Dominy, P.J. Feeney. Experimental and Computational Approaches to Estimate Solubility and Permeability in Drug Discovery and Develop ment Settings. *Adv. Drug Deliv. Rev.* **23** (1997) 3–25.

[4] L.T. Nguyen, J.K. Chau, N.A. Perry, L. de Boer, S.A.J. Zaat, H.J. Vogel. Serum stabilities of short tryptophan- and arginine-rich antimicrobial peptide analogs. *PLoS One* **5** (2010) 1–8.

[5] J.R. North, S. Takenaka, A. Rozek, A. Kielczewska, S. Opal, L.A. Morici, B.B. Finlay, C.J. Schaber, R. Straube, O. Donini. A novel approach for emerging and antibiotic resistant infections: Innate defense regulators as an agnostic therapy. *J. Biotechnol.* **226** (2016) 24–34.

[6] Z. Qian, T. Liu, Y.Y. Liu, R. Briesewitz, A.M. Barrios, S.M. Jhiang, D. Pei. Efficient delivery of cyclic peptides into mammalian cells with short sequence motifs. *ACS Chem. Biol.* **8** (2013) 423–31.

[7]   V. Sebbage. Cell-penetrating peptides and their therapeutic applications. *Biosci. Horizons*, **2** (2009) 64–72.

[8]   R. Trehin, H.P. Merkle. Chances and pitfalls of cell penetrating peptides for cellular drug delivery. *Eur. J. Pharm. Biopharm*. **58** (2004) 209–223.

[9]   J.D. Ramsey, N.H. Flynn. Cell-penetrating peptides transport therapeutics into cells. *Pharmacol. Ther.* **154** (2015) 78–86.

[10] F. Wang, Y Wang, X. Zhang, W. Zhang, S. Guo, F. Jin. Recent progress of cell-penetrating peptides as new carriers for intracellular cargo delivery. *J. Control. Release* **174** (2014) 78–86.

[11] A. Gräslund, F. Madani, S. Lindberg, Ü. Langel, S. Futaki. Mechanisms of cellular uptake of cell-penetrating peptides. *J. Biophys.,* **2011** (2011) 414729.

[12] N. Schmidt, A. Mishra, G.H. Lai, G.C.L. Wong. Arginine-rich cell-penetrating peptides. *FEBS Lett.* **584** (2010) 1806–1813.

[13] K. Valko, C. M. Du, C. Bevan, D. Reynolds, M.H. Abraham. Rapid-gradient HPLC method for measuring drug interactions with immobilised artificial membrane: comparison with other lipophilicity measures. *J. Pharm. Sci*. **89** (2000) 1085–1095.

[14] K.L. Valko, S.P. Teague, C. Pidgeon. In vitro membrane binding and protein binding (IAM MB/PB technology) to estimate in vivo distribution: applications in early drug discovery. *ADMET DMPK* **5** (2017) 14-38.

[15] S.H. Joo. Cyclic peptides as therapeutic agents and biochemical tools. *Biomol. Ther.* **20** (2012) 19–26.

[16] P. Thansandote, R.M. Harris, H.L. Dexter, G.L. Simpson, S. Pal, R.J. Upton, K. Valko. Improving the passive permeability of macrocyclic peptides: Balancing permeability with other physicochemical properties. *Bioorganic Med. Chem.* **23** (2015) 322–327.

[17] J.G. Beck, J. Chatterjee, B. Laufer, M.U. Kiran, A.O. Frank, S. Neubauer, O. Ovadia, S. Greenberg, C. Gilon, A. Hoffman, H. Kessler. Intestinal permeability of cyclic peptides: Common key backbone motifs identified. *J. Am. Chem. Soc.* **134** (2012) 12125–12133.

[18] F. Giordanetto, J. Kihlberg. Macrocyclic drugs and clinical candidates: What can medicinal chemists learn from their properties?. *J. Med. Chem.* **57** (2014) 278–295.

[19] N.C. Tan, P. Yu, Y.U. Kwon, T. Kodadek. High-throughput evaluation of relative cell permeability between peptoids and peptides. *Bioorganic Med. Chem.* **16** (2008) 5853–5861.

[20] B. Testa, P. Crivori, M. Reist, P.A. Carrupt. The influence of lipophilicity on the pharmacokinetic behavior of drugs: Concepts and examples. *Perspect. Drug Discov. Des.* **19** (2000) 179–211.

[21] R. Gulaboski, F. Scholz. Lipophilicity of Peptide Anions: An Experimental Data Set for Lipophilicity Calculations. *J. Phys. Chem. B* (2003) 5650–5657.

[22] A. Visconti, G. Ermondi, G. Caron, R. Esposito. Prediction and interpretation of the lipophilicity of small peptides. *J. Comput. Aided. Mol. Des.* **29** (2015) 361–370.

[23] G. Ermondi, F. Catalano, M. Vallaro, I. Ermondi, M.P. Leal, L. Rinaldi, S. Visentin, G. Caron. Lipophilicity of amyloid β-peptide 12-28 and 25-35 to unravel their ability to promote hydrophobic and electrostatic interactions. *Int. J. Pharm.* **495** (2015) 179–185.

[24] J.L. Meek. Prediction of peptide retention times in high-pressure liquid chromatography on the basis of amino acid composition. *Proc. Natl. Acad. Sci.* **77** (1980) 1632–1636.

[25] K.M. Biswas, D.R. DeVido, J.G. Dorsey. Evaluation of methods for measuring amino acid hydrophobicities and interactions. *J. Chromatogr. A* **1000** (2003) 637–655.

[26] C.T. Mant, R.S. Hodges. Reversed-phase liquid chromatography as a tool in the determination of the hydrophilicity/hydrophobicity of amino acid side-chains at a ligand-receptor interface in the presence of different aqueous environments: II. Effect of varying peptide ligand hydro. *J. Chromatogr. A* **972** (2002) 61–75.

[27] C. Vraka, S. Mijailović, V. Fröhlich, M. Mitterhauser. Expanding LogP: Present possibilities. *Nucl. Med. Biol.* **58** (2013) 20–32.

[28]   K.M. Biswas, D.R. DeVido, J.G. Dorsey. Evaluation of methods for measuring amino acids hydrophobicities and interactions. *J. Chromatogr. A* **1000** (2003) 637-655.

[29]   D. Gussakovsky, H. Neustaeter, V. Spicer, O. Krokhine. Peptide retention time prediction for immobilized artificial K.M. Biswas, D.R. DeVido, J.G. Dorsey. Evaluation of methods for measuring amino acids hydrophobicities and interactions. *J. Chromatogr. A* **1000** (2003) 637-50655membrane phosphatydilcholine stationary phase: method development and preliminary observations. *ADMET DMPK* (2018) doi: http://dx.doi.org/10.5599/admet.520.

[30]   K. Valko. Lipophilicity and biomimetic properties measured by HPLC to support drug discovery. *J. Pharm. Biomed. Anal.* **130** (2016) 35–54.

[31]   F. Tsopelas, C. Giaginis, A. Tsantili-Kakoulidou. Lipophilicity and biomimetic properties to support drug discovery. *Expert Opinion on Drug Discovery* **12** (2017) 885-896.

[32]   K. Valko, C. Du, C. Bevan, D. Reynolds, M. Abraham. Rapid Method for the Estimation of Octanol / Water Partition Coefficient (Log Poct) from Gradient RP-HPLC Retention and a Hydrogen Bond Acidity Term (Sigma alpha2H). *Curr. Med. Chem.* **8** (2001) 1137–1146.

[33]   F. Hollosy, K. Valkó, A. Hersey, S. Nunhuck, G. Kéri, C. Bevan. Estimation of Volume of Distribution in Humans from HPLC Measurements of Human Serum Albumin Binding and Immobilized Artificial Membrane Partitioning. *J. Med. Chem.* **49** (2006) 6958–6971.

[34]   K. Valko, S. Nunhuck, C. Bevan, M.H. Abraham, D.P. Reynolds. Fast Gradient HPLC Method to Determine Compounds Binding to Human Serum Albumin. Relationships with Octanol/Water and Immobilized Artificial Membrane Lipophilicity. *J. Pharm. Sci.* **92** (2003) 2236-2248.

[35]   L.J. Gordon. M. Allen, P. Artursson, M.M. Hann, B.J. Leavens, A. Mateus, S. Readshaw, K. Valko, G.J. Wayne, A. West. Direct Measurement of Intracellular Compound Concentration by RapidFire Mass Spectrometry Offers Insights into Cell Permeability. *J. Biomol. Screen.* **21** (2016) 156-164.

[36]   K. Valko, Physicochemical and biomimetic properties in drug discovery - Chromatographic techniques for lead optimization. Wiley, Hoboken, NJ (2014).

[37]   I. Canals, K. Valkó, E. Bosch, A.P. Hill, M. Rosés. Retention of ionizable compounds on HPLC. 8. Influence of mobile-phase pH change on the chromatographic retention of acids and bases during gradient elution. *Anal. Chem.* **73** (2001) 4937–4945.

[38]   K.L. Valkó, S.B. Nunhuck, A.P. Hill. Estimating Unbound Volume of Distribution and Tissue Binding by in vitro HPLC-based Human Serum Albumin and Immobilized Artificial Artificial Membrane-Binding Measurements. *J. Pharm. Sci.* **100** (2011) 849–862.

[39]   K. Valko, E. Chiarparin, S. Nunhuck, D. Montanari. *In vitro* measurement of drug efficiency index to aid early lead optimization. *J. Pharm. Sci.* **101** (2012) 4155-4169.

[40]   B. I. Díaz-Eufracio, O. Palomino-Hernández, R. A. Houghten, J.L. Medina-Franco. Exploring the chemical space of peptides for drug discovery: a focus on linear and cyclic penta-peptides. *Mol. Divers.* (2018) doi: 10.1007/s11030-018-9812-9.

[41]   V. Stepanić, D. Žiher, V. Gabelica-Marković, D. Jelić, S. Nunhuck, K. Valko, S. Koštrun.. Physicochemical profile of macrolides and their comparison with small molecules. *Eur. J. Med. Chem.* **47** (2012) 462–472.

[42]   K. Valko, M. Kindy, J. Evans, D. Ko. In vitro and in vivo characterization of GM6 an endogenous regulator peptide drug candidate for Amyotrophic Lateral Sclerosis (ALS). *ADMET DMPK* (2018) doi: http://dx.doi.org/10.5599/admet.547.